POLITECNICO DI TORINO
Repository ISTITUZIONALE

Determining Real Permittivity from Fresnel Coefficients in GNSS-R

(Article begins on next page)

25 April 2024

Determining Real Permittivity from Fresnel Coefficients in GNSS-R

Patrizia Savi[1, *], Silvano Bertoldo[1], and Albert Milani[2, 3]

Abstract—Global Navigation Satellite System Reflectometry (GNSS-R) can be used to derive information about the composition or the properties of ground surfaces, by analyzing signals emitted by GNSS satellites and reflected from the ground. If the received power is measured with linearly polarized antennas, under the condition of smooth surface, the reflected signal is proportional to the modulus of the perpendicular and parallel polarization Fresnel coefficients, which depend on the incidence angle θ, and on the dielectric constant ε of the soil. In general, ε is a complex number; for non-dispersive soils, the imaginary part of ε can be neglected, and a real value of ε is sought. We solve the real-valued problem explicitly giving formulas that can be used to determine the dielectric constant ε and we compare the analytical solution with experimental data in the case of sand soil.

1. INTRODUCTION

Global Navigation Satellite System Reflectometry (GNSS-R) is a technique for sensing the Earth surface, based on the principle of detecting GNSS signals reflected off the ground, and processing them to monitor its properties remotely (see [1]). This application is a key input in the areas of ocean observation (see e.g., [2]), ice (see e.g., [3, 4]) and land remote sensing (see e.g., [5–7]), altimetry (see e.g., [8, 9]), climate modeling and weather prediction [10]. The passive bi-static radar configuration used in this technique requires no transmitters except GNSS satellites, thus enabling the system to be light and compact (see e.g., [11–14]). The Signal to Noise (SNR) data recorded by GNSS receivers are related to the direct signals and those reflected by the ground. Under the assumption that the surface be flat, and considering a receiving antenna either vertically or horizontally polarized, the SNR is related to the Fresnel reflection coefficients for vertical and horizontal polarization, which are functions of the relative permittivity of the soil and of the incident angle [15]. The relative permittivity of the soil is generally obtained by solving the Fresnel coefficient equations numerically; then, the soil moisture can be obtained by applying several well established models (see for example the semi-empirical models of [16, 17]). These models may be useful for the monitoring of a field of known characteristics in terms of sand, clay percentage, etc. In more general cases, i.e., for non-flat surfaces, more powerful techniques of inverse scattering should be used [18].

2. STATEMENT OF THE PROBLEM

The total electromagnetic field received by the down-looking antenna is the sum of various signals, scattered by the Earth's surface (see Fig. 1). These are essentially of two kinds: coherent and incoherent [19]. If the surface is approximately smooth, the non-coherent component is negligible, and the total power received by the antenna can be approximated by the coherent part only [5].
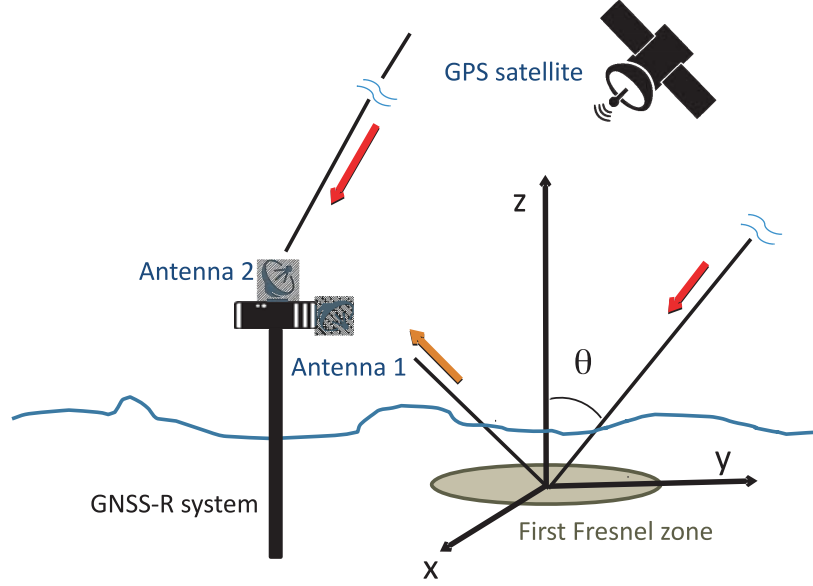
Figure 1. GNSS reflectometry geometry.

The coherent component in the GPS bistatic radar is given by

$$P_{pol,\,coh} = R_{pol}\frac{P_t G_t G_r \lambda^2}{(4\pi)^2 (r_1 + r_2)^2}, \tag{1}$$

where the product $P_t G_t$ is the Equivalent Isotropic Radiated Power (EIRP) of the transmitted signal; G_r is the receiver antenna gain; λ is the wavelength ($\lambda = 19.042\,\text{cm}$ for GPS L1 signal); r_1 and r_2 are, respectively, the distance between the receiver and the specular point, and that between the specular point and satellite; R_p is the power reflectivity of the reflecting surface at a specified polarization (*pol*). For smooth surfaces, the reflectivity can be approximated by

$$R_{pol} = |\Gamma_{pol}|^2, \tag{2}$$

where Γ_{pol} is the Fresnel reflection coefficient. In the case of perpendicular (or horizontal, or TE) polarization and parallel (or vertical, or TM) polarization, the corresponding Fresnel reflection coefficients can be written, respectively, as:

$$\Gamma_n = \frac{\cos\theta - \sqrt{\varepsilon - \sin^2\theta}}{\cos\theta + \sqrt{\varepsilon - \sin^2\theta}}, \qquad \Gamma_p = \frac{\varepsilon\cos\theta - \sqrt{\varepsilon - \sin^2\theta}}{\varepsilon\cos\theta + \sqrt{\varepsilon - \sin^2\theta}}. \tag{3}$$

As mentioned in [20], our goal is to find the value of the permittivity ε from these two relations. For general media, including in particular dispersive ones, ε is a complex number and can be found from Equation (3), interpreted as a system of two equations in the two unknowns $\Re(\varepsilon)$ and $\Im(\varepsilon)$. For non-dispersive media, ε is a real number, and can be found from either of the two relations in Eq. (3), which can be solved individually, and explicitly, for real ε. Thus, one can choose to carry out the measurements relative to either the perpendicular or the parallel case. As we show, the first equation of Eq. (3) (i.e., the perpendicular case) is much simpler to solve; on the other hand, the measurements of Γ_p may point to the evidence of the so-called Brewster angle θ_B, in which case the determination of ε is immediate. While the simplest expression $\varepsilon_p = \tan^2\theta_B$ is well known, it is in practice quite difficult if not impossible to use it; hence, the merit of alternative formulas such as the ones we describe here. At any rate, one needs to be sure that the value of ε determined by either equation is the same, and also independent of the particular value of θ at which the measurement is taken; this can happen only if the angle and the coefficients satisfy a mutual compatibility condition, which can also be described (and, therefore, checked) explicitly. In the sequel, we clarify these remarks in the particular situation in which we have measurements of the moduli $\gamma_n = |\Gamma_n|$ and $\gamma_p = |\Gamma_p|$, as per Eq. (2). We provide explicit, real solutions to Eq. (3), and compare our results with those of [18] for dry sand. This method can be generalized to equations of similar kind.

3. THE FRESNEL INVERSE PROBLEM

We look for real solutions $\varepsilon > 1$ (to signify that the medium is denser than air) to either the equation

$$\left| \frac{\cos\theta - \sqrt{\varepsilon - \sin^2\theta}}{\cos\theta + \sqrt{\varepsilon - \sin^2\theta}} \right| = |\Gamma_n| =: \gamma_n, \tag{4}$$

or

$$\left| \frac{\varepsilon\cos\theta - \sqrt{\varepsilon - \sin^2\theta}}{\varepsilon\cos\theta + \sqrt{\varepsilon - \sin^2\theta}} \right| = |\Gamma_p| =: \gamma_p, \tag{5}$$

with $\theta \in [0, \frac{\pi}{2}[$ and, correspondingly, $0 < \gamma_p \leq \gamma_n < 1$ (these conditions are necessarily satisfied if Eqs. (4) and (5) do have a common solution). Then, Equation (4) has a unique solution $\varepsilon_n > 1$, given by

$$\varepsilon_n = 1 + \frac{4\gamma_n \cos^2\theta}{(1 - \gamma_n)^2}. \tag{6}$$

This solution is constant under certain compatibility conditions between γ_n and θ similar to Eq. (15), in the sense that ε is independent of the particular angle θ at which the values of γ_n is measured. The determination of an explicit, constant solution of Eq. (5) is more complicated. We assume that there is $\theta_B \in]\frac{\pi}{4}, \frac{\pi}{2}[$, corresponding to which $\gamma_p = 0$ (θ_B is the Brewster angle; this too is a necessary condition for solvability). We define

$$\lambda_p := \frac{1 + \gamma_p}{1 - \gamma_p} \geq 1, \tag{7}$$

and note that $\lambda_p = 1$ only when $\gamma_p = 0$. We define further

$$\mu_p := \begin{cases} \lambda_p & \text{if} \quad 0 \leq \theta \leq \theta_B, \\ \dfrac{1}{\lambda_p} & \text{if} \quad \theta_B \leq \theta < \dfrac{\pi}{2} \end{cases} \tag{8}$$

(recall that $\lambda_p = \frac{1}{\lambda_p} = 1$ at θ_B), and

$$\theta_1 := \begin{cases} \dfrac{\pi}{2} & \text{if} \quad \tan^2\theta_B \geq 2, \\ \arcsin\left(\dfrac{1}{\sqrt{2}}\tan\theta_B\right) & \text{if} \quad \tan^2\theta_B < 2. \end{cases} \tag{9}$$

Then, Equation (5) has a solution $\varepsilon_p > 1$, given by

$$\varepsilon_p = \frac{\mu_p}{2\cos^2\theta}\left(\mu_p + \text{sgn}(\theta_1 - \theta)\sqrt{\mu_p^2 - \sin^2(2\theta)}\right). \tag{10}$$

This solution is obtained by patching together three different solutions ε_p^0, defined on all of $[0, \frac{\pi}{2}[$, and ε_p^1, ε_p^2, defined only in $[\theta_B, \frac{\pi}{2}[$, as long as $\lambda_p \sin(2\theta) \leq 1$ in this interval. The three solutions are given by:

$$\varepsilon_p^0 = \frac{\lambda_p^2}{2\cos^2\theta}\left(1 + \sqrt{1 - \frac{\sin^2(2\theta)}{\lambda_p^2}}\right), \tag{11}$$

$$\varepsilon_p^1 = \frac{1}{2\lambda_p^2\cos^2\theta}\left(1 + \sqrt{1 - \lambda_p^2\sin^2(2\theta)}\right), \tag{12}$$

$$\varepsilon_p^2 = \frac{1}{2\lambda_p^2\cos^2\theta}\left(1 - \sqrt{1 - \lambda_p^2\sin^2(2\theta)}\right). \tag{13}$$

In principle, these solutions depend on θ, and satisfy the conditions:

$$\varepsilon_p^0 \geq \tan^2\theta \geq \varepsilon_p^1 \geq 2\sin^2\theta \geq \varepsilon_p^2 \geq 1. \tag{14}$$
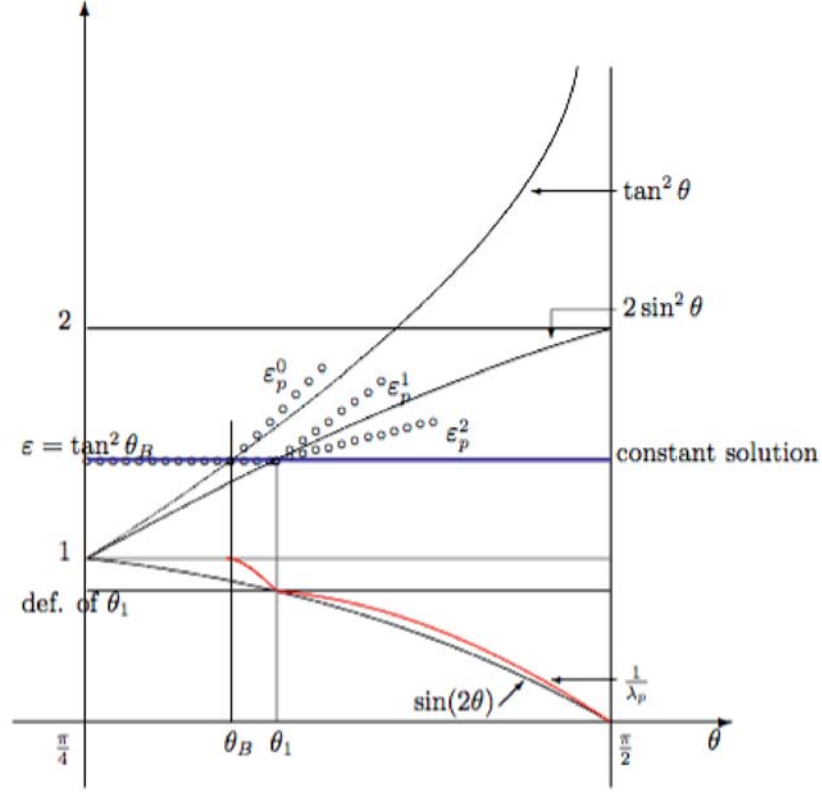
Figure 2. Solution of (5). On $[\frac{\pi}{4}, \theta_B]$, $\varepsilon = \tan^2 \theta_B = \varepsilon_p^0$; on $[\theta_B, \theta_1]$, $\varepsilon = \tan^2 \theta_B = \varepsilon_p^1$; on $[\theta_1, \frac{\pi}{2}[$, $\varepsilon = \tan^2 \theta_B = \varepsilon_p^2$.

We find that the constant solution to the Fresnel formulas is given by $\varepsilon_p = \tan^2 \theta_B$ (as is well known); however, ε_p^0 can be constant only if θ varies between $\frac{\pi}{4}$ and θ_B, because, after θ_B, $\varepsilon_p^0 > \tan^2 \theta_B^2$. Likewise, ε_p^1 can be constant only when θ varies between θ_B and θ_1, because, after θ_1, $\varepsilon_p^1 > 2\sin^2 \theta > \tan^2 \theta_B$. On the other hand, ε_p^2 can be constant for θ between θ_1 and $\frac{\pi}{2}$, because $\tan^2 \theta_B < \varepsilon_p^2 < 2\sin^2 \theta$ (see Fig. 2).

The solutions ε_n and ε_p coincide on all of $[0, \frac{\pi}{2}[$ if and only if the compatibility condition:

$$\lambda_n^2 \cos^2 \theta + \sin^2 \theta = \lambda_n \mu_p \tag{15}$$

holds in $[0, \frac{\pi}{2}[$, where, as in Eq. (7),

$$\lambda_n := \frac{1 + \gamma_n}{1 - \gamma_n} > 1, \tag{16}$$

together with the additional conditions $\gamma_p \le \gamma_n^2$, if $\theta_B \le \theta \le \theta_1$, or $\gamma_n^2 \le \gamma_p$, if $\theta_1 \le \theta < \frac{\pi}{2}$. In this case, the common solution $\varepsilon_n = \varepsilon_p =: \varepsilon_c$ is given by

$$\varepsilon_c = \lambda_n \mu_p, \tag{17}$$

and ε_c is constant on $[0, \frac{\pi}{2}[$; in fact, as mentioned above,

$$\varepsilon_c = \tan^2 \theta_B. \tag{18}$$

We note that the only cases in which the identity $\gamma_n^2 = \gamma_p$ can hold for some $\tilde{\theta}$, together with the compatibility condition (15), are: $\tilde{\theta} = \frac{\pi}{4}$ if $\tilde{\theta} \in [0, \theta_B[$, or $\tilde{\theta} = \theta_1$ (defined in Eq. (9)) if $\tilde{\theta} \in [\theta_B, \frac{\pi}{2}[$, in

which case $\varepsilon = 2\sin^2\theta_1 = 2\lambda_n^2/(1 + \lambda_n^2)$. More precisely, the case $\theta = \frac{\pi}{4}$ and $\gamma_n^2 = \gamma_p$ is exceptional, in that Equations (4) and (5) are identities in ε; that is, *any* $\varepsilon \in \mathbb{R}$ (in fact, any $\varepsilon \in \mathbb{C}$) is a solution.

The reflected GPS signals are predominantly LH [5], especially for satellites with high elevation (angles greater than 60°). Using the Subscript LR to represent the scattering when a satellite incident signal (right-hand polarized) is scattered by the surface and inverts the polarization to the left-hand, the reflection coefficient, Γ_{LR}, can be written as a linear combination of vertical and horizontal polarization [15]:

$$\Gamma_{LR} = \frac{1}{2}(\Gamma n - \Gamma p) \tag{19}$$

Note that:

$$\gamma_n = \frac{1}{2}(|\Gamma n - \Gamma p| + |\Gamma n + \Gamma p|) \tag{20}$$

$$\gamma_p = \frac{1}{2}||\Gamma n - \Gamma p| - |\Gamma n + \Gamma p|| \tag{21}$$

If $\theta = 0°$, then $\Gamma_n = -\Gamma_p$, therefore:

$$\gamma_n = \frac{1}{2}|\Gamma n - \Gamma p| = |\Gamma_{LR}| \tag{22}$$

$$\gamma_p = \gamma_n \tag{23}$$

The values of signal to noise ratio (SNR) can be obtained from the GNSS-R measurements considering various satellites with different elevation angles. Considering the satellites with high elevation angles (i.e., $\theta \sim 0$), the SNR values the amplitude of the reflection coefficient $|\Gamma_{LR}|$ can be obtained and the value of permittivity evaluated from 10.

4. RESULTS

As a first example, in Fig. 3 we consider the measurements of $|\Gamma_n|$ and $|\Gamma_p|$ reported in [18] for a medium composed of sand, for which $\varepsilon = 3 + \sigma j$, with $|\sigma| \leq 0.05$. We compute the values of ε_n and ε_p predicted by Eqs. (6) and (10), as well as the common value $\varepsilon_c = \lambda_n\lambda_p$.

We find that these values match the approximate value $\varepsilon \approx 3$ with error not exceeding 1%. The measurements of $|\Gamma_p|$ point to the evidence of a possible Brewster angle at approximately $\theta_B = 60°$ (which would be the exact value for $\varepsilon = 3$). The relative error is given by $e_c := \frac{1}{3}|\varepsilon_c - 3|$ (see Fig. 4).
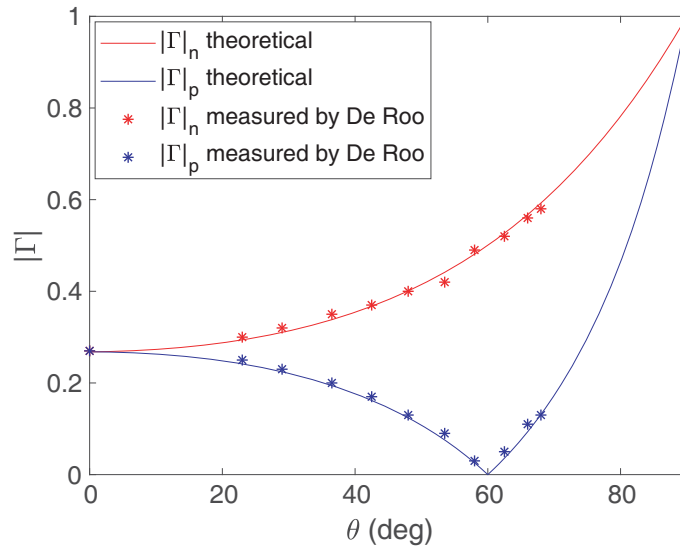

Figure 3. Measurements of $|\Gamma_n|$ and $|\Gamma_p|$ reported in [18] (solid line) and data evaluated from (6) and (10) (dots).
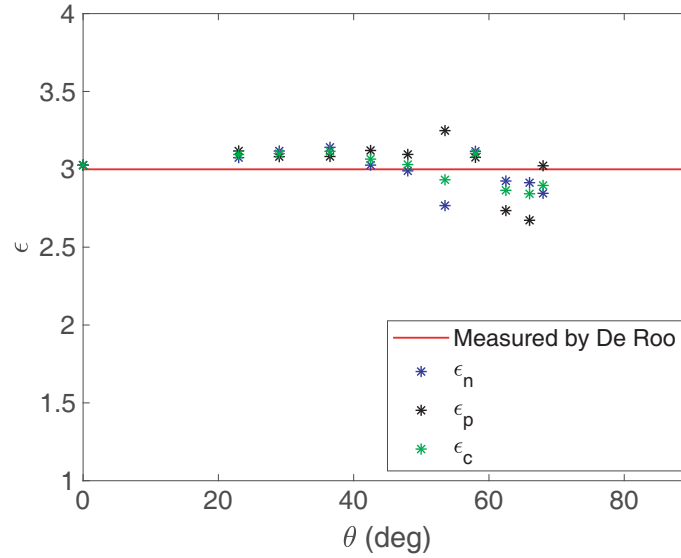
Figure 4. Relative error.

As a second example, we consider some GNSS-R measurements carried out in a controlled environment located in Grugliasco, Torino (450358.5N, 73533.8E). In this location, a wide field of known characteristics (mainly 50% sand) belonging to the Interuniversity Department of Regional and Urban Studies and Planning (DIST), Politecnico di Torino, is available. The composition of the terrain is reported in Table 1. In this campaign, the direct GPS signals were measured using a right-hand circular polarized (RHCP) antenna, while the reflected signals were measured with a left-hand circular polarized (LHCP) antenna. The complete description of the setup can be found in [21]. In addition to the GNSS-R measurements, Time-Domain Reflectometry (TDR) measurements were carried out to be used as reference. An average value of about 6.4 was obtained for the permittivity. In Fig. 5, the magnitude of the two reflection coefficients is reported for $\epsilon = 6.4$. In particular, for a permittivity value equal to 6.4, for an elevation angle higher than 80° (corresponding to an incidence angle θ less than 20°), the difference between $|\Gamma_n|$ and $|\Gamma_n|$ is less than 0.043. In this case, the real permittivity can be obtained by using formula (10) for $|\Gamma_p|$.

The results of the GNSS measurements and the computation of the permittivity values are reported in Table 2. Only satellite PRN 9 is considered because of its elevation. It can be observed that the values with an elevation angle greater than 80° are close to the results obtained with the TDR technique.

Table 1. Composition of the soil for the Grugliasco experiment.

Coarse sand (%)	Fine sand (%)	Very Fine sand (%)
115.5	50.1	16.1

Coarse silt (%)	Fine silt (%)	Clay (%)	Organic matter(%)
5.3	8.2	4.8	1.4

Table 2. Computation of the permittivity values from the measurements.

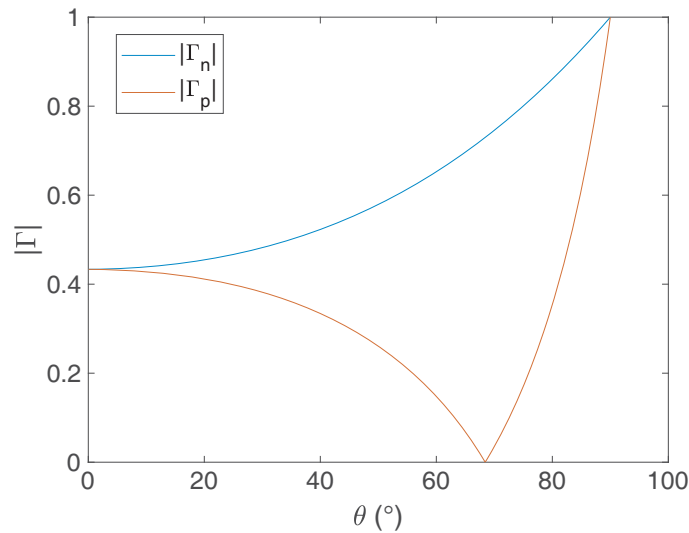| Elevation (deg)	θ (deg)	SNR (dB)	$|\Gamma_{LR}|$	ϵ
82.4	7.6	11	0.195	6.57
83.2	6.8	13	0.195	6.59

Figure 5. Amplitude of reflection coefficients for $\epsilon = 6.4$.

5. CONCLUSIONS

In GNSS-R for soil moisture applications, one essentially needs to determine the permittivity ε of the soil from the Fresnel coefficients. For non-dispersive soil, ε can be assumed real. In the literature, ε is mostly found numerically. In fact, Equations (4) and (5) can be explicitly solved. We determine real solutions with $\varepsilon > 1$, for all angles $\theta \in [0, \frac{\pi}{2}[$ and all measurements γ_n, $\gamma_p \in]0, 1[$, with $\gamma_p \leq \gamma_n$, which satisfy the compatibility conditions (15).

Our results suggest two possible strategies to determine the solution. The first hinges on being able to find a value $\gamma_p \approx 0$ at a particular position $\tilde{\theta}$; then, $\tilde{\theta}$ is an approximation of the Brewster angle, and the approximate solution is simply $\varepsilon \approx \tan^2 \tilde{\theta}$, as per Eq. (18). Otherwise, one can take any angle θ in $[0, \frac{\pi}{4}[$, and verify that the corresponding measurements of γ_n and γ_p satisfy condition (15). If so, the solution is $\varepsilon = \lambda_n \lambda_p$, as per Eq. (17).

ACKNOWLEDGMENT

REFERENCES

1. Jin, S., E. Cardellach, and F. Xie, *GNSS Remote Sensing: Theory, Methods and Applications*, Springer, 2014.
2. Zavorotny, V. U. and A. G. Voronovich, "Scattering of GPS signals from the ocean with wind remote sensing application," *IEEE Transactions on Geoscience and Remote Sensing*, Vol. 38, No. 2, 951–964, March 2000.
3. Wiehl, M., B. Legrésy, and R. Dietrich, "Potential of reflected GNSS signals for ice sheeet remote sensing," *Progress In Electromagnetics Research*, Vol. 40, 177–205, 2003.
4. Alonso-Arroyo, A., V. U. Zavorotny, and A. Camps, "Sea ice detection using U.K. TDS-1 GNSS-R data," *IEEE Transactions on Geoscience and Remote Sensing*, Vol. 55, No. 9, 4989–5001, 2017.
5. Masters, D., A. Penina, and S. Katzberg, "Initial results of land-reflected GPS bistatic radar measurements in SMEX02," *Remote Sensing of Environment*, Vol. 92, No. 4, 507–520, 2004.

6. Ban, W., K. Yu, and X. Zhang, "GEO-satellite-based reflectometry for soil moisture estimation: Signal modeling and algorithm development," *IEEE Transactions on Geoscience and Remote Sensing*, Vol. 56, No. 3, 1829–1838, 2018.

7. Pierdicca, N., A. Mollfulleda, F. Costantini, L. Guerriero, L. Dente, S. Paloscia, E. Santi, and M. Zribi, "Spaceborne GNSS reflectometry data for land applications: An analysis of techdemosat data," *International Geoscience and Remote Sensing Symposium (IGARSS)*, 3343–3346, Valencia, Spain, July 22–27, 2018.

8. Li, W., A. Rius, F. Fabra, E. Cardellach, S. Ribó, and M. Martín-Neira, "Revisiting the GNSS-R waveform statistics and its impact on altimetric retrievals," *IEEE Transactions on Geoscience and Remote Sensing*, Vol. 56, No. 5, 2854–2871, 2018.

9. Mashburn, J., P. Axelrad, S. T. Lowe, and K. M. Larson, "Global ocean altimetry with GNSS reflections from TechDemoSat-1," *IEEE Transactions on Geoscience and Remote Sensing*, Vol. 56, No. 7, 4088–4097, July 2018.

10. Cardellach, E., et al., "GNSS Transpolar Earth Reflectometry exploriNg System (G-TERN): Mission concept," *IEEE ACCESS*, Vol. 6, 13980–14018, 2018, DOI: 10.1109/ACCESS.2018.2814072.

11. Katzberg, S., O. Torres, M. Grant, and D. Masters, "Utilizing calibrated GPS reflected signals to estimate soil reflectivity and dielectric constant: Results from SMEX02," *Remote Sensing of Environment*, Vol. 100, 17–28, 2005.

12. Egido, A., M. Caparrini, G. Ruffini, S. Paloscia, E. Santi, L. Guerriero, N. Pierdicca, and N. Floury, "Global navigation satellite systems reflectometry as a remote sensing tool for agriculture," *Remote Sensing*, Vol. 4, 2356–2372, 2012.

13. Yu, K., C. Rizos, D. Burrage, A. G. Dempster, K. Zhang, and M. Markgraf, "An overview of GNSS remote sensing," *EURASIP Journal on Advances in Signal Processing*, 2014–2134, 2014.

14. Pei, Y., R. Notarpietro, P. Savi, and F. Dovis, "A fully software GNSS-R receiver for soil monitoring," *International Journal of Remote Sensing*, Vol. 35, No. 6, 2378–2391, 2014.

15. Stutzman, W. L., *Polarization in Electromagnetic Systems*, Artech House, 1993.

16. Wang, J. and T. Schmugge, "An empirical model for the complex dielectric permittivity of soils as a function of water content," *IEEE Transactions on Geoscience and Remote Sensing*, Vol. 18, No. 4, 288–295, 1980.

17. Hallikainen, A. and F. Ulaby, "Microwave dielectric behavior of wet soil — Part 1: Empirical models and experimental observations," *IEEE Transactions on Geoscience and Remote Sensing*, Vol. 23, No. 1, 25–34, Jan. 1985.

18. Roo, R. D. and F. Ulaby, "Bistatic specular scattering from rough dielectric surfaces," *IEEE Transactions on Antennas and Propagation*, Vol. 42, No. 2, 220–231, 1994.

19. Pierdicca, N., L. Guerriero, M. Brogioni, and A. Egido, "On the coherent and non coherent components of bare and vegetated terrain bistatic scattering: Modelling the GNSS-R signal over land," *Proc. IEEE Int. Geosci. Remote Sens. Symp.*, 3407–3410, Munich, Germany, July 22–27, 2012.

20. Savi, P. and A. Milani, "Real-valued solutions to an inverse Fresnel problem in GNSS-R," *Inernational Geoscience and Remote Sensing Symposium (IGARSS2018)*, 3327–3330, Valencia, Spain, July 22–27, 2018.

21. Jia, Y., P. Savi, D. Canone, and R. Notarpietro, "Estimation of surface characteristics using GNSS LH-reflected Signals: Land versus water," *IEEE Journal of Selected Topics in Applied Earth Observations and Remote Sensing*, Vol. 9, No. 10, 4752–4758, Oct. 2016.